Journal of Molecular Structure 1153 (2018) 149–156

Contents lists available at ScienceDirect

Journal of Molecular Structure

journal homepage: http://www.elsevier.com/locate/molstruc

Three VO^{2+} complexes of the pyridoxal-derived Schiff bases: Synthesis, experimental and theoretical characterizations, and catalytic activity in a cyclocondensation reaction

Faezeh Jafari-Moghaddam [a], S. Ali Beyramabadi [a, *], Maryam Khashi [b], Ali Morsali [a]

[a] Department of Chemistry, Mashhad Branch, Islamic Azad University, Mashhad, Iran
[b] Young Researchers and Elite Club, Mashhad Branch, Islamic Azad University, Mashhad, Iran

ARTICLE INFO

Article history:
Received 1 July 2017
Received in revised form
14 September 2017
Accepted 2 October 2017
Available online 3 October 2017

Keywords:
Oxovanadium
Schiff base
Pyridoxal
DFT
Catalyst
Cyclocondensation reaction

ABSTRACT

Three oxovanadium(IV) complexes of the pyridoxal Schiff bases have been newly synthesized and characterized. The used Schiff bases were N,N′-dipyridoxyl(ethylenediamine), N,N′-dipyridoxyl(1,3-propanediamine) and N,N′-dipyridoxyl(1,2-benzenediamine). Also, the optimized geometry, assignment of the IR bands and the Natural Bond Orbital (NBO) analysis of the complexes have been computed using the density functional theory (DFT) methods. Dianionic form of the Schiff bases ($\mathbf{L}^{2-}$) acts as a tetradentate N_2O_2 ligand. The coordinating atoms of the Schiff base are the phenolate oxygens and imine nitrogens, which occupy four base positions of the square-pyramidal geometry of the complexes. The oxo ligand occupies the apical position of the [VO(**L**)] complexes. In the optimized geometry of the complexes, the coordinated Schiff bases have more planar structure than their free form. Due to the high-energy gaps, all of the complexes are predicted to be stable. Good agreement between the experimental values and the DFT-computed results supports suitability of the optimized geometries for the complexes. The investigated complexes show high catalytic activities in synthesis of the tetrahydrobenzo[*b*]pyrans through a three-component cyclocondensation reaction of dimedone, malononitrile and some aromatic aldehydes. The complexes catalyzed the reaction in solvent free conditions and the catalysts were found to be reusable.

1. Introduction

Due to selectivity and sensitivity towards the metallic ions, the Schiff bases are of great importance in coordination chemistry [1–4]. In addition, the Schiff bases and their complexes show important role in a variety of areas such as catalyst [5], photochemistry [6] and especially various biological activities including antibacterial [7,8], antifungal [8–10], antimicrobial [11,12], antidiabetic [10,13] and in treatment of a broad spectrum of cancers [8,14,15].

Vanadium compounds exhibit significant role in biological systems such as treatment of type II diabetes [16,17]. Some of the vanadium complexes mimic the insulin [18–20]. Also, oxovanadium(IV) complexes of the Schiff bases exhibit biological activities such as insulin enhancing properties [13,21–23]. In addition to the antidiabetic activities, many vanadium complexes show important biological properties such as the anticancer [20,24–28], antimicrobial [29–31] and spermicidal activities [32].

The pyridoxal is a close analogue of pyridoxine (Vitamin B_6) [33], acts as a cofactor in many enzymatically-catalyzed-biosynthetic process such as transamination [34], dehydration of serine and threonine, decarboxylation and racemization of amino acids [35]. The pyridoxal has anticancer activity [36,37]. Its metallic complexes have displayed several biological activities such as antiproliferative agent [38,39]. Metal complexes of the pyridoxal Schiff bases play important role in identification of the mechanism of action of the pyridoxal as well as developing compounds with biological applications such as the anticancer agents [40,41]. Vanadium complexes of the pyridoxal Schiff bases exhibit important biological activities such as phosphatase inhibitor [42], antimicrobial [43] and antioxidant [44] agent. Vanadium complexes of the Schiff bases with N and O donor sites exhibit insulin enhancing properties [13,45], too. Since, vanadium complexes of the pyridoxal

---

* Corresponding author.
E-mail addresses: beiramabadi@yahoo.com, beiramabadi6285@mshdiau.ac.ir (S.A. Beyramabadi).

https://doi.org/10.1016/j.molstruc.2017.10.007

Schiff bases are particularly interesting in this regard. It is expected that the use of the pyridoxal Schiff base yield no toxic metabolites and improve solubility of the final complex. Based on these reasons, we report synthesis and experimentally characterization of three new V(IV) complexes of the Schiff bases derived from the pyridoxal. The used Schiff bases were N,N′-dipyridoxyl(ethylenediamine) [= $\mathbf{H_2L1}$], N,N′-dipyridoxyl(1,3-propanediamine) [= $\mathbf{H_2L2}$] and N,N′-dipyridoxyl(1,2-benzenediamine) [= $\mathbf{H_2L3}$]. The V(IV) complexes of these Schiff bases are named as the [VO(**L1**)], [VO(**L2**)] and [VO(**L3**)], respectively. In addition, geometry optimization, theoretical assignment of the IR spectra as well as the NBO analyses of the complexes have been computed by using the DFT methods. Computed structural parameters of the complexes and assignment of their vibrational-IR frequencies can be useful in identification of the similar compounds, too.

Because of high atom economy and high selectivity, the multicomponent reactions are of great importance in modern organic synthesis and medicinal chemistry. These reactions are used in synthesis of significant organic molecules and effective biological compounds from simple materials [46–51]. The vanadium complexes are known to be active as catalyst in organic reactions [52–54]. Catalytic activity of the vanadium complexes of the pyridoxal Schiff bases in organic synthesis has been reported, previously [55]. Another aim of this work is usage of the synthesized oxovanadium(IV) complexes as the catalyst in a three-component cyclocondensation reaction.

2. Experimental

2.1. Material and methods

The three used Schiff bases were synthesized as we reported previously, $\mathbf{H_2L1}$ [56], $\mathbf{H_2L2}$ [57] and $\mathbf{H_2L3}$ [58]. Other used chemicals were obtained from the Merck Company, which were used without any further purification. The melting points were determined using an electrothermal 9100 melting point apparatus. The IR spectra were recorded on a Bruker Tensor 27 spectrophotometer from KBr disks. The elemental analysis for C, H and N were performed on a Heraeus elemental analyzer CHN–*O*-Rapid. Percentage of the V^{2+} metal ion of the complexes was measured by using a Hitachi 2–2000 atomic absorption spectrophotometer. Also, the mass spectra were recorded on a Shimadzu-GC-Mass-Qp 1100 Ex, where the used method was atmospheric pressure chemical ionization.

2.2. Synthesis of the oxovanadium(IV) complexes

0.5 mmol of the $\mathbf{H_2L}$ Schiff-base ligand was dissolved in 15 mL methanol. Then, 1 mmol of the NEt_3 base was added to solution of the ligand. A solution of 0.5 mmol (1.265 g) of $VO(SO_4)\cdot 5H_2O$ in 10 mL methanol was added slowly to solution of the Schiff-base. The mixture was stirred for 3 h in 40–50 °C. Color of the obtained precipitates for the [VO(**L1**)] and [VO(**L2**)] complexes were green, while the [VO(**L3**)] one is dark-orange. The precipitates were filtered off, washed with methanol and dried in oven. Yields of the [VO(**L1**)], [VO(**L2**)] and [VO(**L3**)] complexes were 67, 63 and 71%, respectively and their melting points were 230.2, 220.1 and 226.3 °C, respectively.

3. Computational details

Theoretical calculations including the geometries optimization, frequency calculations and the NBO analyses have been carried out with the UB3LYP functional [59] as implemented in the Gaussian 03 program [60]. The 6-311 + G(d,p) basis set was used except for the vanadium atom, where the LANL2DZ basis set [61] was employed with considering its the effective core potential functions.

The full-optimized geometries do not show any imaginary frequencies, confirming that the optimized structures represent a true local minimum in the potential energy surface. The optimized geometries of the complexes were employed to calculate their vibrational frequencies and the NBO analyses. The DFT-predicted vibrational frequencies are usually higher than the experimental values. Since, we used the scale factor of 0.9614 for correction of the calculated frequencies [62]. The NBO analysis of the investigated complexes were done to identify their frontier orbitals and exploring important bond orders. All structures were visualized by employing the Chemcraft 1.7 program [63].

4. Results and discussion

In this work, three complexes of the pyridoxal Schiff bases have been synthesized and characterized by various techniques. The elemental analysis results of the complexes are gathered in Table 1. These data confirms the [VO(**L**)] formula for all of the complexes, where the dianionic $\mathbf{L}^{2-}$ Schiff base is coordinated to the V^{4+} metal ion. In the mass spectra of the VO(**L1**)], [VO(**L2**)] and [VO(**L3**)] complexes, the molecular ion peaks, m/z (M^+), were observed at 423, 437 and 471, respectively. These molecular ion peaks are in consistent with the proposed formula weights for the complexes, confirming correctness of the proposed formulas for three investigated complexes. Based on the CHN analysis, percentage of the V^{4+} metal ion and the molecular ion peaks, the 1:1 ratio of the $\mathbf{L^{2-}}$ ligand and V^{4+} metal ion is proposed in structure of the investigated complex as the [VO(**L**)] formula.

4.1. Geometry optimization

As mentioned in previous section, the [VO(**L**)] formula was proposed for the investigated complexes, where the $\mathbf{L}^{2-}$ can act as a tetradentate ligand. Geometries of the investigated complexes have been optimized, which are shown in Fig. 1. Also, their structural parameters are listed in Table S1 in the Supplementary Material file. The optimized geometries and structural parameters of the $\mathbf{H_2L1}$, $\mathbf{H_2L2}$ and $\mathbf{H_2L3}$ free Schiff bases have reported in Refs. [56–58], respectively. For comparison, the optimized geometry and structural parameters of the $\mathbf{H_2L3}$ Schiff base are given in Fig. 2 and Table S1, respectively. None of the three Schiff bases has a planar optimized geometry, but two pyridine rings are in a separate plane and make approximately a 40° dihedral angle to each other. However, in comparison with the free $\mathbf{H_2L}$ ligands, the coordinated $\mathbf{L^{2-}}$ ligand shows a more planar structure in the optimized geometries of the complexes. For example, the calculated C6–N2–N4–C10, O1–O2–N4–N2, N1–C2–C9–N3 and C5–C3–C8–C11 dihedral angles of the free $\mathbf{H_2L}$ Schiff base ligands are about −150, −150 and −130°, respectively, which are about 0° for the [VO(**L**)] complexes (Table S1).

For complexation, the $\mathbf{H_2L}$ ligand is firstly deprotonated. Then, the dianionic $\mathbf{L}^{2-}$ species acts as a tetradentate ligand. Two deprotonated phenolate oxygens (O1 and O2 atoms) and two azomethine nitrogens (N2 and N4 atoms) are four coordinating atoms of the investigated Schiff base ligands. In the square-pyramidal geometry of the V(IV) complexes, these four donor atoms lie in the same plane, occupy four coordinating positions of the square base (Fig. 1). It is noticeable that the V^{4+} ion is not in the same plane with the donor atoms of the Schiff base, where the calculated O1–O2–N4–V and O1–N2–N4–V dihedral angles are about 25°. The apex position of the complexes is occupied with the oxo ligand (O5). As seen in Table S1, the V–O5 bond length is significantly lower than the V–O1 and V–O2 ones.

Table 1
The elemental analysis of the investigated oxovanadium(IV) complexes.

Compound	Calculated (%)				Found (%)			
	C	H	N	Vanadium	C	H	N	Vanadium
[VO(**L1**)]= $C_{18}H_{20}N_4O_5V$	51.07	4.76	13.24	12.03	50.84	5.03	13.61	11.58
[VO(**L2**)]= $C_{19}H_{22}N_4O_5V$	52.18	5.07	12.81	11.65	51.67	4.59	13.43	10.99
[VO(**L3**)]= $C_{22}H_{20}N_4O_5V$	56.06	4.28	11.89	10.81	55.62	5.31	11.52	10.70

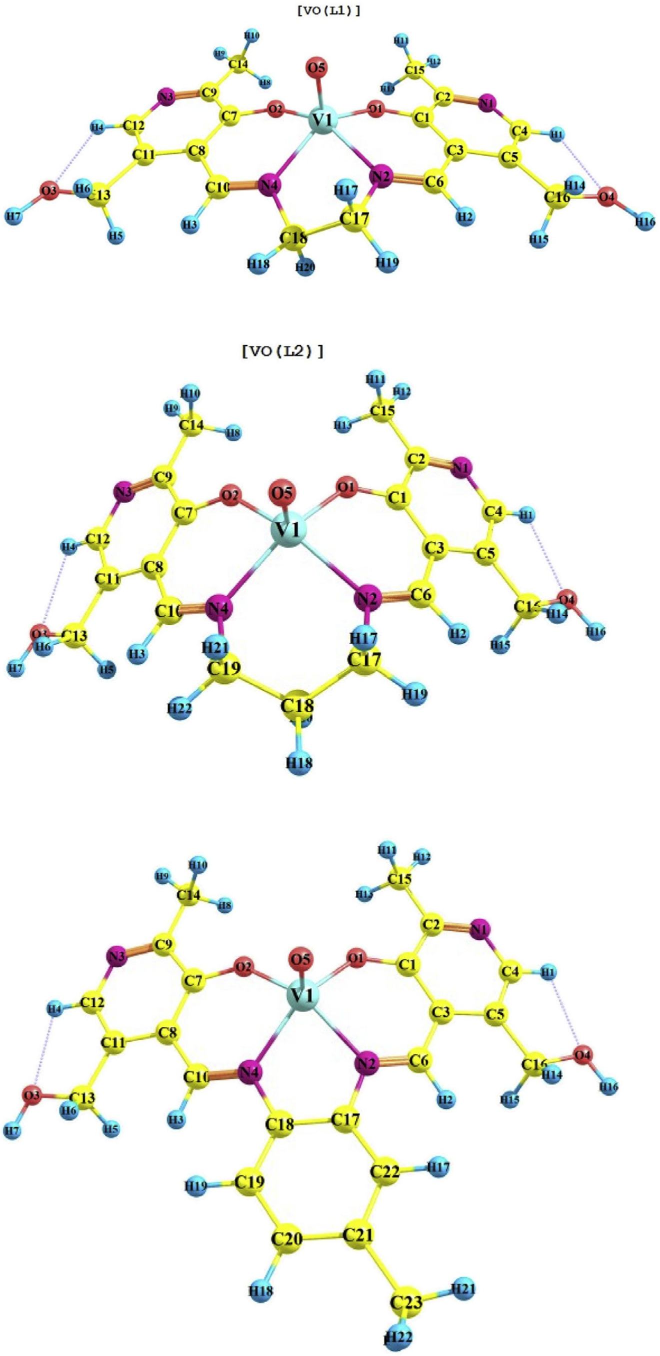

Fig. 1. Optimized geometries of the investigated oxovanadium(IV) complexes together with their labeling.

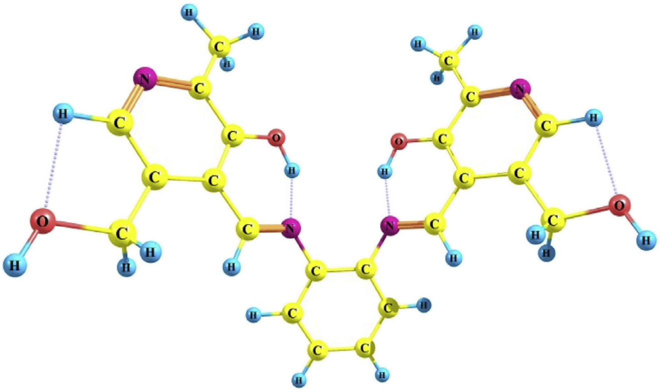

Fig. 2. Optimized geometry of the H_2**L3** free Schiff base.

Rotations around the C17—N2 and C18—N4 single bonds provide structural necessities for the complex formation, which put the two sides of the L^{2-} species in the same plane. In the free H_2**L** Schiff bases, the calculated C1—O1—O2 and C6—N2—N4 angles are about 140° [56–58], which are 160–170° for the V(IV) complexes, respectively. Also, the calculated C6—N2—C17—C18 and C6—N2—C17—C22 dihedral angle of the free H_2**L3** ligand are 138.4 and 43.3°, respectively, which are −160.0 and 22.2° for the [VO(**L3**)] complex, respectively.

The computed C=C and C=N bond lengths of the aromatic rings are in the expectable range [13,31,44,55–58,64–69]. The pyridine-C bond lengths for the $-CH_2OH$ and $-CH_3$ substitutions are about 150 pm, which are appropriate sizes for the pyridine-carbon bonds. All of the substituted groups as well as the azomethine moieties are essentially in the same plane with the pyridine rings (Table S1).

In comparison with the free H_2**L** Schiff bases, coordination of the N2 and N4 azomethine nitrogens to the V^{4+} ion results in elongation of the C6=N2 and C10 = N4 bonds. While, the C1—O1 and C7—O2 bond lengths are decreased in the complexes. Deprotonation of the phenolic oxygens causes to a decrease in theses bond lengths. The DFT-computed structural parameters for the investigated complexes are good in agreement with the reported values for the similar compounds [13,31,43–45,55–58,64–69].

4.2. Vibrational spectroscopy

Theoretical assignment of the spectra is a useful tool in identification of the chemical compounds. In this research, the vibrational modes of the synthesized complexes have been analyzed by comparing their experimental and DFT-predicted IR frequencies. The experimental and theoretical IR spectra of the three investigated complexes are given in the Supplementary Material file. Three investigated complexes show essentially a similar IR spectrum. Since, important vibrational frequencies of the [VO(**L3**)] complex are only gathered in Table 2 together with the selected vibrational frequencies of its ligand, the H_2**L3** Schiff base, for comparison. Selected IR frequencies of the [VO(**L1**)] and [VO(**L2**)] complexes are discussed in text, too.

Table 2
Selected experimental and calculated IR vibrational frequencies (cm^{-1}) of the **H_2L3** Schiff base and its [VO(**L3**)] complex.

Experimental frequencies		Calculated frequencies				Vibrational assignment
H_2L3	[VO(L3)]	H_2L3	IR Intensity ($km.mol^{-1}$)	[VO(L3)]	IR Intensity ($km.mol^{-1}$)	
	538 (m)			526	139	$\upsilon_{asym}(O1{-}V{-}O3)+\upsilon_{asym}(N1{-}V{-}N4)$
	650 (w)			725, 652	29, 39	$\upsilon(V{-}O, V{-}N)$ of the L1 ligand
752 (m)	765 (m)	743	34	735	66	$\delta_{op}(C{-}H)$ aromatic
838 (w)		813	118	–	–	$\delta_{ip}(O{-}H)$ phenolic
	969 (s)	963	69	984	93	$\upsilon_{sym}(py\text{-}C{-}O)_{alc}$
		1021	94	1033	72	$\upsilon_{asym}(py\text{-}C{-}O)_{alc}$
	1016 (m)	–	–	1029	170	$\upsilon(V{-}O5)$
1026(s)	1096 (m)	1058	136	1064	102	$\upsilon(C7{-}O2)+\upsilon(C22{-}O4)$
1208 s)	1191 (s)	1176	147	1171	248	$\upsilon(C{=}C, C{=}N)$ of the aromatic rings+ $\upsilon(C15{-}N1, C13{-}N4)$
1261 (m)	1276 (s,sh)	1266	60	1288	109	$\upsilon(C{=}C, C{=}N)$ of the aromatic rings+ $\upsilon(py\text{-}C)$
1298 (s)	1320 (s)	1342	68	1384	67	$[\delta_{wag}(CH_2)+\delta_{ip}(OH)]alc$
		1357	74	1378	115	$\upsilon(py\text{-}C)$
1384 (vs)	1399 (vs)	1369	198	1402	213	$\upsilon(C{-}O)$ phenolic
1476 (m)	1512 (m)	1550	93	1551	31	$\upsilon(C{=}C)$ of the benzene ring
1615 (vs)	1576 (s,sh)	1572	57	1555	247	$\upsilon(C2{-}O1, C17{-}O3)+\upsilon(C{=}C, C{=}N)$ of the pyridine rings
	1603 (vs)	1659	239	1642	318	$\upsilon(C21{-}N4)+\upsilon(C4{-}N1)$
		2877	37	2844	64	$\upsilon_{sym}(CH)_{alc}$
2497 (m)		2916	16	2917	22	$\upsilon_{asym}(CH)$ Me
2606 (s)		2935	13	2865	60	$\upsilon_{asym}(CH_2)_{alc}$
2833 (s)		2952	37	3012	17	$\upsilon(C4{-}H1)+\upsilon(C21{-}H19)$
2945 (s,br)	2916 (s,br)	3016, 2961	13, 20	3016,	9,	$\upsilon_{asym}(CH)$ Me
3175 (s,br)	3144 (s,br)	3073–3048	46, 32, 14	3091–3063	4–13	$\upsilon(C{-}H)$ aromatic
		3078, 3063	468, 299	–	–	$\upsilon(O{-}H)$ phenolic
		3674	38	3708	80	$\upsilon(O{-}H)_{alc}$

Abbreviation:wag, wagging; op, out-of-plane; ip, in-plane; alc, substituted $-CH_2OH$ groups; w, weak; m, medium; s, strong; vs, very strong; sh, shoulder.

In the IR spectra of the Schiff bases, a very intensive band at 1660-1500 cm^{-1} region is related to the C=N stretching vibration of the azomethine group [58,64–66,68–76]. The symmetrical stretching modes of C6=N2 and C10 = N4 bonds result in a very intensive band at 1640, 1632 and 1615 cm^{-1} of the IR spectra of the **H_2L1**, **H_2L2** and **H_2L3** Schiff bases, respectively. These intensive bands shift to lower frequencies in the IR spectra of the complexes, appear at 1626, 1626 and 1603 cm^{-1} of the IR spectra of the [VO(**L1**)], [VO(**L2**)] and [VO(**L3**)] complexes, respectively. This confirms coordination of the **L^{2-}** ligands *via* the azomethine nitrogens (N2 and N4 atoms), which reduces electron density and bonding order of the C6=N2 and C10 = N4 bonds [56–58,64–66,75,76].

In the 3600-2000 cm^{-1} region of the IR spectra, overlapping of the O–H, N–H and C–H stretching vibration modes causes to band broading [56–58,64–66,70,75–77]. Assignment of this spectral region of the [VO(**L3**)] complex is given in Table 2. As seen, the most intensive band of the complexes is related to the stretching vibrations of the alcoholic O–H bonds.

Deprotonation of the phenolic oxygens increases the electron density in the bonding region of the C1–O1 and C7–O2 bonds. Since, the C1–O1 and C7–O2 stretching vibrations of the complexes appear at higher frequencies than the corresponding free Schiff bases. The phenolic υ(C–O) vibrations result in a very strong band at 1388, 1387 and 1384 $cm^{-1}$of the IR spectra of the **H_2L1**, **H_2L2** and **H_2L3** free Schiff bases, respectively, which appear at 1401, 1402 and 1399 cm^{-1} of the IR spectra of the [VO(**L1**)], [VO(**L2**)] and [VO(**L3**)] complexes, respectively.

4.3. NBO analysis

The NBO analysis has been shown various applications such as investigation of atomic charges, molecular orbitals, charge transfer of the chemical compounds and so on [56–58,64,66,74]. Shapes of the highest-occupied-molecular orbital (HOMO) and the lowest-unoccupied-molecular orbital (LUMO) are similar for all of the

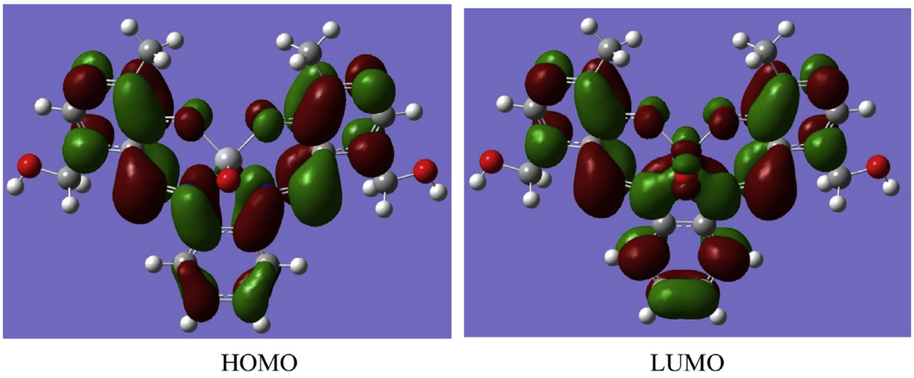
HOMO LUMO

Fig. 3. The HOMO and LUMO frontier orbitals of the [VO(**L3**)].

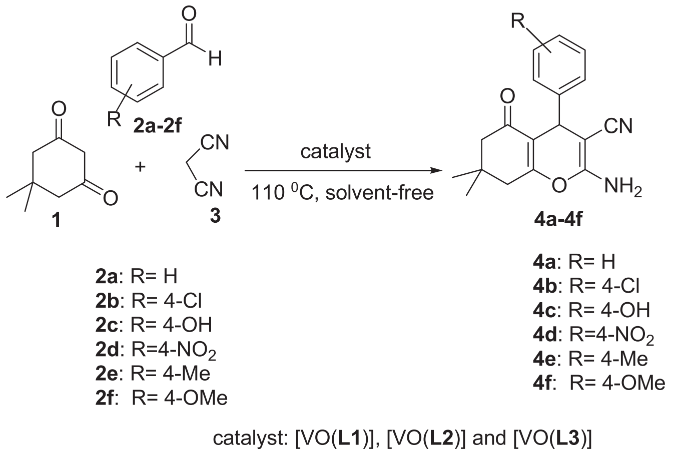

Scheme 1. The V(IV) complexes catalyzed the synthesis of the tetrahydrobenzo[*b*] pyran derivatives.

Table 3
Effect of the catalyst amount and temperature on the model reaction.

Entry	Catalyst (g)	T (°C)	Time (min)	Yields (%) in presence of the catalysts		
				[VO(L1)]	[VO(L2)]	[VO(L3)]
1	–	120	240	–	–	–
2	0.01	100	30	71	78	70
3	0.01	110	15	78	80	76
4	0.01	120	20	80	81	80
5	0.03	100	30	75	83	73
6	0.03	110	15	83	83	80
7	0.03	120	20	85	85	83
8	0.05	100	30	88	87	86
9	0.05	110	15	90	90	90
10	0.05	120	20	90	90	90
11	0.07	110	15	90	90	90

three investigated V(IV) complexes. For example, the 3D-shapes of the HOMO and LUMO orbitals of the [VO(**L3**)] complex are shown in Fig. 3.

Both of the HOMO and LUMO orbitals of the complexes are mainly localized on the aromatic rings and the azomethine groups. The VO moiety contributes only in the LUMO orbital. The $-CH_3$ and $-CH_2OH$ substitutions of the pyridine rings have no role in the frontier orbitals (Fig. 3).

The energy difference between the HOMO and LUMO orbitals plays essential role in photochemical reactions, electric properties and electronic spectra of the chemical compounds. The calculated-energy gap for the [VO(**L1**)], [VO(**L2**)] and [VO(**L3**)] complexes are 3.21, 3.21 and 3.13 eV, respectively. These large energy gaps between the frontier orbitals confirm high stability of the investigated complexes [56–58,64,66,74,78].

The NBO analysis shows that the bond order of the C6=N2 and C10 = N4bonds decreases from 1.68 in the free **H_2L3** ligand to 1.47 in the [VO(**L3**)] complex. But, the C1–O1 and C7–O2 bond order increases from 1.12 in the **H_2L3** to 1.30 for the [VO(**L3**)] complex. These results are good in agreement with the IR spectral data. In comparison with the free **H_2L3** Schiff base, the C=N stretching vibrational mode of azomethine groups shifts to the lower energies, but the phenolic C–O stretching vibration shifts to higher energies in the IR spectrum of the [VO(**L3**)] complex.

4.4. Catalytic performance of the V (IV) complexes

Based on the catalytic activities of the vanadium complexes [52–55] and importance of the multicomponent reactions in organic synthesis [50,51], we have utilized three synthesized vanadium(IV) complexes as catalyst in a three-component cyclocondensation reaction of dimedone **1**, aromatic aldehydes 2**a**-2**f** and malononitrile **3** to give the tetrahydrobenzo[*b*]pyrans 4**a**-4**f** (Scheme 1).

For the preparation of the tetrahydrobenzo[*b*]pyrans **4a-4f**, a mixture of dimedone **1** (1 mmol), aryl aldehydes **2a-2f** (1 mmol) and malononitrile **3** (1 mmol), and a catalytic amount of the V(IV) complex was heated in an oil bath in the appropriate temperature and time (Table 3). The reaction was monitored by the TLC. Upon completion of the transformation, the reaction mixture was cooled to room temperature and boiling ethanol was added. This resulted in the precipitation of the catalyst, which was collected by filtration. The product was collected from the filtrate after cooling to the room temperature and recrystallized from ethanol in high yields.

To optimize the reaction conditions, dimedone **1** (1 mmol), benzaldehyde **2a** (1 mmol) and malononitrile **3** (1 mmol) were selected as model reaction in different sets of conditions and the best results are summarized in Table 3. We used the catalysts in the various solvents such as H_2O, CH_2Cl_2, CH_3CN and EtOH; but the product yield was very low. Therefore, we utilized the complexes in the solvent-free conditions. As seen in Table 3, without any catalyst even after prolonged reaction time, no product was observed (entry 1). The best results both in terms of time and yield were obtained when the reaction was conducted without solvent at 110 °C in the presence of 0.05 g of [VO(**L1**)], [VO(**L2**)] and [VO(**L3**)] as the catalyst (entry 9).

To evaluate the generality of this method, the scope of the reaction was investigated with a variety of aromatic aldehydes under optimized reaction conditions (Table 3, Entry 9). The obtained results are presented in Table 4.

The [VO(**L**)] catalysts could be readily recovered from the reaction mixture. We found that the catalysts could be used again with only a slight reduction in activity. The structural retention of the catalysts was confirmed by comparing the FT-IR spectra of the recovered catalysts with the its fresh form (Fig. 4).

Table 4
The catalytic synthesis of the tetrahydrobenzo[*b*]pyran derivatives **4a-4f by** using the [VO(**L**)] complexes as the catalyst.

Entry	Ar	Product	Time (min)	Yields (%) in the presence of the catalysts			m.p. (°C)	
				[VO(L1)]	[VO(L2)]	[VO(L3)]	Found	Reported [79]
1	C_6H_5	**4a**	15	90	90	90	230–231	230
2	$4\text{-}ClC_6H_4$	**4b**	15	95	90	93	208–209	206
3	$4\text{-}OHC_6H_4$	**4c**	20	85	80	83	208–210	210
4	$4\text{-}MeC_6H_4$	**4d**	10	90	87	91	216–218	218
5	$4\text{-}NO_2C_6H_4$	**4e**	15	89	80	86	175–177	177
6	$4\text{-}OMeC_6H_4$	**4f**	10	93	88	90	204–206	203

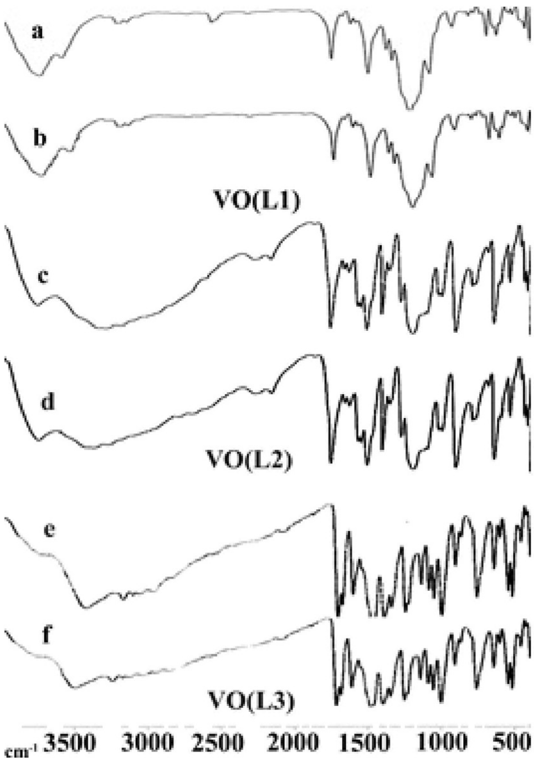

Fig. 4. The FT-IR spectra of fresh catalysts (**a, c, e**) and the recovered catalysts (**b, d, f**) for the synthesis of the species **4a**.

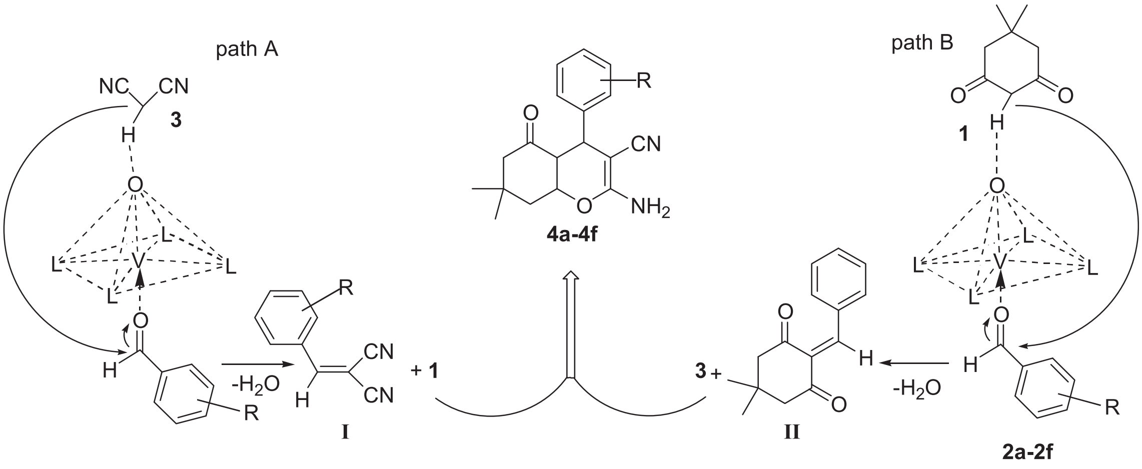

Scheme 2. A plausible mechanism for the formation of benzo[*b*]pyrans in the presence of the V(IV) complexes as the catalyst.

A plausible mechanism for this reaction is provided in Scheme 2. It is reasonable to assume that the V(IV) complexes can play a dual role [47]. Thus, we propose that the vanadium ion induces the polarization of the carbonyl group of the species **2**, whereas the oxygen atoms are slightly basic in the vanadium complexes and can activate the reactants (species **1** and **3**) and also the intermediates in this reaction. As shown in Scheme 2, the product, species **4**, may be formed either through the path A or through the path B. We propose that the V(IV) complexes facilitate catalytically the formation of the intermediates **I** and **II**, which subsequently react together to give the final products **4a-4f**.

5. Conclusion

In this work, three oxovanadium(IV) complexes of the pyridoxal Schiff bases have been newly synthesized and characterized experimentally and theoretically. The complexes have the [VO(**L**)] formula, where the dianionic $\mathbf{L}^{2-}$ of the $\mathbf{H_2L}$ Schiff base acts as a tetradentate ligand. Two phenolate oxygens and two azomethine nitrogens are donating atoms of the Schiff bases, occupy four coordination positions of the base in the square-planar geometry of the complexes. The Schiff bases show more planar structure in optimized geometry of the complexes than their free forms. The vanadium atom is shifted from the square plane upward the deprotonated $\mathbf{L}^{2-}$ ligand. The apical position of the complexes is occupied by the oxo ligand.

There is good consistency between the calculated structural parameters of the complexes and the reported values for the similar compounds. The IR-frequencies of the investigated complexes have been assigned theoretically. Good agreement between the experimental-IR frequencies and the DFT-calculated frequencies support suitability of the optimized geometries for the complexes, too. The high HOMO-LUMO energy gaps approve stability of the complexes.

The synthesized complexes were used as a catalyst in a three-component-cyclocondensation reaction of the dimedone and malononitrile with various aryl aldehydes to produce the tetrahydrobenzo[*b*]pyrans. In various solvent, no valuable yield of the product was observed. The optimum reaction conditions for the benzaldehyde as a reactant is 0.05 g of the catalyst, $T = 110\,^{\circ}C$ and $t = 15$ min in free solvent condition.

Appendix A. Supplementary data

Supplementary data related to this article can be found at https://doi.org/10.1016/j.molstruc.2017.10.007.

References

[1] E. Keskioğlu, A.B. Gündüzalp, S. Cete, F. Hamurcu, B. Erk, Cr (III), Fe (III) and Co (III) complexes of tetradentate (ONNO) Schiff base ligands: synthesis, characterization, properties and biological activity, Spectrochim. Acta. Part A 70 (2008) 634–640.

[2] H. Sharghi, M.A. Nasseri, Schiff-base metal (II) complexes as new catalysts in the efficient, mild and regioselective conversion of 1, 2-epoxyethanes to 2-

hydroxyethyl thiocyanates with ammonium thiocyanate, Bull. Chem. Soc. Jpn. 76 (2003) 137–142.

[3] U.C. Saha, K. Dhara, B. Chattopadhyay, S.K. Mandal, S. Mondal, S. Sen, M. Mukherjee, S. van Smaalen, P. Chattopadhyay, A new half-condensed Schiff base compound: highly selective and sensitive pH-responsive fluorescent sensor, Org. Lett. 13 (2011) 4510–4513.

[4] M. Shakir, M. Azam, Y. Azim, S. Parveen, A.U. Khan, Synthesis and physico-chemical studies on complexes of 1, 2-diaminophenyl-N, N′-bis-(2-pyridinecarboxaldimine)(L): a spectroscopic approach on binding studies of DNA with the copper complex, Polyhedron 26 (2007) 5513–5518.

[5] K. Gupta, A. Sutar, Polymer anchored Schiff base complexes of transition metal ions and their catalytic activities in oxidation of phenol, J. Mol. Catal. A Chem. 272 (2007) 64–74.

[6] U. McDonnell, M.R. Hicks, M.J. Hannon, A. Rodger, DNA binding and bending by dinuclear complexes comprising ruthenium polypyridyl centres linked by a bis (pyridylimine) ligand, J. Inorg. Biochem. 102 (2008) 2052–2059.

[7] A.B. Gündüzalp, İ. Özsen, H. Alyar, S. Alyar, N. Özbek, Biologically active Schiff bases containing thiophene/furan ring and their copper (II) complexes: synthesis, spectral, nonlinear optical and density functional studies, J. Mol. Struct. 1120 (2016) 259–266.

[8] A.K. Abu Al-Nasr, R.M. Ramadan, Spectroscopic studies and biological activity of some transition metal complexes of unusual Schiff base, Spectrochim. Acta. Part A 105 (2013) 14–19.

[9] W. Singh, B. Dash, Synthesis of some new Schiff bases containing thiazole and oxazole nuclei and their fungicidal activity, Pesticides 22 (1988) 33–37.

[10] A. Rauf, A. Shah, A.A. Khan, A.H. Shah, R. Abbasi, I.Z. Qureshi, S. Ali, Synthesis, pH dependent photometric and electrochemical investigation, redox mechanism and biological applications of novel Schiff base and its metallic derivatives, Spectrochim. Acta. Part A 176 (2017) 155–167.

[11] A.A. Abdel Aziz, F.M. Elantabli, H. Moustafa, S.M. El-Medani, Spectroscopic, DNA binding ability, biological activity, DFT calculations and non linear optical properties (NLO) of novel Co(II), Cu(II), Zn(II), Cd(II) and Hg(II) complexes with ONS Schiff base, J. Mol. Struct. 1141 (2017) 563–576.

[12] A.-N.M.A. Alaghaz, Y.A. Ammar, H.A. Bayoumi, S.A. Aldhlmani, Synthesis, spectral characterization, thermal analysis, molecular modeling and antimicrobial activity of new potentially N2O2 azo-dye Schiff base complexes, J. Mol. Struct. 1074 (2014) 359–375.

[13] T. Mukherjee, J.O. Costa Pessoa, A. Kumar, A.R. Sarkar, Oxidovanadium (IV) schiff base complex derived from vitamin B6: synthesis, characterization, and insulin enhancing properties, Inorg. Chem. 50 (2011) 4349–4361.

[14] M. Shebl, Synthesis, spectroscopic characterization and antimicrobial activity of binuclear metal complexes of a new asymmetrical Schiff base ligand: DNA binding affinity of copper (II) complexes, Spectrochim. Acta. Part A 117 (2014) 127–137.

[15] S. Desai, P. Desai, K. Desai, Synthesis of some Schiff bases, thiazolidinones and azetidinones derived from 2, 6-diaminobenzo [1, 2-d: 4, 5-d'] bisthiazole and their anticancer activities, Heterocycl. Commun. 7 (2001) 83–90.

[16] K.H. Thompson, C. Orvig, Vanadium in diabetes: 100 years from phase 0 to phase I, J. Inorg. Biochem. 100 (2006) 1925–1935.

[17] Y. Shechter, I. Goldwaser, M. Mironchik, M. Fridkin, D. Gefel, Historic perspective and recent developments on the insulin-like actions of vanadium; toward developing vanadium-based drugs for diabetes, Coord. Chem. Rev. 237 (2003) 3–11.

[18] K.H. Thompson, J. Lichter, C. LeBel, M.C. Scaife, J.H. McNeill, C. Orvig, Vanadium treatment of type 2 diabetes: a view to the future, J. Inorg. Biochem. 103 (2009) 554–558.

[19] K.H. Thompson, C. Orvig, Metal Complexes in Medicinal Chemistry: New Vistas and Challenges in Drug Design, Dalton Trans, 2006, pp. 761–764.

[20] A. Levina, A.I. McLeod, A. Pulte, J.B. Aitken, P.A. Lay, Biotransformations of antidiabetic vanadium prodrugs in mammalian cells and cell culture media: a xanes spectroscopic study, Inorg. Chem. 54 (2015) 6707–6718.

[21] D. Sanna, V. Ugone, M. Serra, E. Garribba, Speciation of potential anti-diabetic vanadium complexes in real serum samples, J. Inorg. Biochem. 173 (2017) 52–65.

[22] K. Ghasemi, F. Ghasemi, A.R. Rezvani, C. Graiff, B. Notash, Potential antidiabetic drugs of metformin with insulin-enhancing anions [VO2(dipic)]− and [VO2(dipic-OH)]−: synthesis, characterization and X-ray crystal structure, Polyhedron 102 (2015) 239–245.

[23] M.M. Ibrahim, M.A. Mohamed, G.A.M. Mersal, S. Al-Juaid, Insulin-like action of novel metformin-containing vanadate as a new antidiabatic drug: synthesis, characterization and crystal structure of [Metformin-H]2[V2O6]]·H2O, J. Mol. Struct. 1098 (2015) 92–100.

[24] I. Kostova, Titanium and vanadium complexes as anticancer agents, Anti-Cancer Agents Med. Chem. 9 (2009) 827–842 (Formerly Current Medicinal Chemistry-Anti-Cancer Agents).

[25] A. Papaioannou, M. Manos, S. Karkabounas, R. Liasko, A.M. Evangelou, I. Correia, V. Kalfakakou, J.C. Pessoa, T. Kabanos, Solid state and solution studies of a vanadium (III)-L-cysteine compound and demonstration of its antimetastatic, antioxidant and inhibition of neutral endopeptidase activities, J. Inorg. Biochem. 98 (2004) 959–968.

[26] G. Abdelhamid, A. Anwar-Mohamed, O.A. Badary, A.A. Moustafa, A.O. El-Kadi, Transcriptional and posttranscriptional regulation of CYP1A1 by vanadium in human hepatoma HepG2 cells, Cell Biol. Toxicol. 26 (2010) 421–434.

[27] C. Rozzo, D. Sanna, E. Garribba, M. Serra, A. Cantara, G. Palmieri, M. Pisano, Antitumoral effect of vanadium compounds in malignant melanoma cell lines, J. Inorg. Biochem. 174 (2017) 14–24.

[28] A. Sinha, K. Banerjee, A. Banerjee, S. Das, S.K. Choudhuri, Synthesis, characterization and biological evaluation of a novel vanadium complex as a possible anticancer agent, J. Organomet. Chem. 772 (2014) 34–41.

[29] C. Datta, D. Das, P. Mondal, B. Chakraborty, M. Sengupta, C.R. Bhattacharjee, Novel water soluble neutral vanadium(IV)–antibiotic complex: antioxidant, immunomodulatory and molecular docking studies, Eur. J. Med. Chem. 97 (2015) 214–224.

[30] M. AP, S. Monika, Synthesis, structural, and biological studies of some schiff bases and their metal complexes, Met. Base. Drugs 2008 (2008).

[31] H. Amiri Rudbari, M.R. Iravani, V. Moazam, B. Askari, M. Khorshidifard, N. Habibi, G. Bruno, Synthesis, characterization, X-ray crystal structures and antibacterial activities of Schiff base ligands derived from allylamine and their vanadium(IV), cobalt(III), nickel(II), copper(II), zinc(II) and palladium(II) complexes, J. Mol. Struct. 1125 (2016) 113–120.

[32] Y. Dong, R.K. Narla, E. Sudbeck, F.M. Uckun, Synthesis, X-ray structure, and anti-leukemic activity of oxovanadium (IV) complexes, J. Inorg. Biochem. 78 (2000) 321–330.

[33] J.M. Berg, J.L. Tymoczko, L. Stryer, Biochemistry, WH Freeman and Company, New York, 2002.

[34] P.P. Cohen, Transamination in pigeon breast muscle, Biochem. J. 33 (1939) 1478.

[35] C. Yanofsky, J.L. Reissig, L-Serine dehydrase of Neurospora, J. Biol. Chem. 202 (1953) 567–577.

[36] F. Prior, Theoretical involvement of vitamin B6 in tumour initiation, Med. Hypotheses 16 (1985) 421–428.

[37] V. Herbert, The role of vitamin B12 and folate in carcinogenesis, Adv. Exp. Med. Biol. 206 (1986) 293–311.

[38] V.M. Leovac, M.D. Joksović, V. Divjaković, L.S. Jovanović, Ž. Šaranović, A. Pevec, Synthesis, spectroscopic and X-ray characterization of a copper (II) complex with the Schiff base derived from pyridoxal and aminoguanidine: NMR spectral studies of the ligand, J. Inorg. Biochem. 101 (2007) 1094–1097.

[39] H. Brurok, J.H. Ardenkjær-Larsen, G. Hansson, S. Skarra, K. Berg, J.O. Karlsson, I. Laursen, P. Jynge, Manganese dipyridoxyl diphosphate: MRI contrast agent with antioxidative and cardioprotective Properties?: in vitroandex VivoAssessments, Biochem. Biophys. Res. Commun. 254 (1999) 768–772.

[40] M. Soltani, M. Homayouni-Tabrizi, S. Afsharnezhad, S.A. Beyramabadi, M. Khashi, Evaluation of anti-proliferative and proapoptotic effects of Mn2+ complex of the N, N′-dipyridoxyl (1, 2-diaminobenzene) schiff base against human breast cancer cells (MCF7), J. Cell. Immunother. 1 (2015) 18–19.

[41] B. Annaraj, M.A. Neelakantan, Synthesis, crystal structure, spectral characterization and biological exploration of water soluble Cu(II) complexes of vitamin B6 derivative, Eur. J. Med. Chem. 102 (2015) 1–8.

[42] J.D. Siqueira, A.C.O. Menegatti, H. Terenzi, M.B. Pereira, D. Roman, E.F. Rosso, P.C. Piquini, B.A. Iglesias, D.F. Back, Synthesis, characterization and phosphatase inhibitory activity of dioxidovanadium(V) complexes with Schiff base ligands derived from pyridoxal and resorcinol, Polyhedron 130 (2017) 184–194.

[43] T. Rosu, E. Pahontu, M. Reka-Stefana, D.-C. Ilies, R. Georgescu, S. Shova, A. Gulea, Synthesis, structural and spectral studies of Cu(II) and V(IV) complexes of a novel Schiff base derived from pyridoxal, Antimicrob. Act. Polyhedron 31 (2012) 352–360.

[44] S.A. Elsayed, A.M. Noufal, A.M. El-Hendawy, Synthesis, structural characterization and antioxidant activity of some vanadium(IV), Mo(VI)/(IV) and Ru(II) complexes of pyridoxal Schiff base derivatives, J. Mol. Struct. 1144 (2017) 120–128.

[45] K. Kawabe, T. Suekuni, T. Inada, K. Yamato, M. Tadokoro, Y. Kojima, Y. Fujisawa, H. Sakurai, Syntheses, structures, and insulin-like activities of oxovanadium (IV) complexes with tetra-and penta-dentate histidine derivatives, Chem. Lett. 27 (1998) 1155–1156.

[46] A. Dömling, Recent developments in isocyanide based multicomponent reactions in applied chemistry, Chem. Rev. Wash. D.C. U. S.) 106 (2006) 17–89.

[47] A. Davoodnia, M. Khashi, N. Tavakoli-Hoseini, Tetrabutylammonium hexatungstate [TBA2][W6O19]: novel and reusable heterogeneous catalyst for rapid solvent-free synthesis of polyhydroquinoline via unsymmetrical Hantzsch reaction, Chin. J. Catal. 34 (2013) 1173–1178.

[48] Z. Long, M. Liu, R. Jiang, Q. Wan, L. Mao, Y. Wan, F. Deng, X. Zhang, Y. Wei, Preparation of water soluble and biocompatible AIE-active fluorescent organic nanoparticles via multicomponent reaction and their biological imaging capability, Chem. Eng. J. 308 (2017) 527–534.

[49] J. Yang, X.-W. Liu, D.-D. Wang, M.-Y. Tian, S.-N. Han, T.-T. Feng, X.-L. Liu, R.-Q. Mei, Y. Zhou, Diversity-oriented one-pot multicomponent synthesis of spirooxindole derivatives and their biological evaluation for anticancer activities, Tetrahedron 72 (2016) 8523–8536.

[50] T. Ahmadi, G. Mohammadi Ziarani, P. Gholamzadeh, H. Mollabagher, Recent advances in asymmetric multicomponent reactions (AMCRs), Tetrahedron Asymmetry 28 (2017) 708–724.

[51] Z. Zhou, M. Liu, S. Sun, E. Yao, S. Liu, Z. Wu, J.-T. Yu, Y. Jiang, J. Cheng, Multicomponent reactions (MCRs) of arylmethyl bromides, arylamidines and elemental sulfur toward unsymmetric 3,5-diaryl 1,2,4-thiadiazoles, Tetrahedron Lett. 58 (2017) 2571–2573.

[52] M. Sutradhar, A.J.L. Pombeiro, Vanadium Complexes in Catalytic Oxidations, Reference Module in Chemistry, Molecular Sciences and Chemical Engineering, Elsevier, 2017.

[53] M. Mirzaee, B. Bahramian, M. Mirebrahimi, Amine-functionalized boehmite nanoparticle-supported molybdenum and vanadium complexes: efficient catalysts for epoxidation of alkenes, Chin. J. Catal. 37 (2016) 1263–1274.

[54] P.A. Petrov, A.I. Smolentsev, A.S. Bogomyakov, S.N. Konchenko, Novel vanadium complexes supported by a bulky tris(pyrazolyl)borate ligand, Polyhedron 129 (2017) 60–64.

[55] J. Pisk, J.-C. Daran, R. Poli, D. Agustin, Pyridoxal based ONS and ONO vanadium(V) complexes: structural analysis and catalytic application in organic solvent free epoxidation, J. Mol. Catal. A Chem. 403 (2015) 52–63.

[56] S. Beyramabadi, A. Morsali, S. Vahidi, M. Khoshkholgh, A. Esmaeili, N, N′-dipyridoxyl (ethylenediamine) schiff-base ligand and its square-pyramidal copper (II) complex: synthesis, experimental and theoretical characterization, J. Struct. Chem. 53 (2012) 460–467.

[57] H. Eshtiagh-Hosseini, M.R. Housaindokht, S.A. Beyramabadi, S. Beheshti, A.A. Esmaeili, M.J. Khoshkholgh, A. Morsali, Synthesis, experimental and theoretical characterization of tetra dentate N, N′-dipyridoxyl (1, 3-propylenediamine) salen ligand and its Co (III) complex, Spectrochim. Acta. Part A 71 (2008) 1341–1347.

[58] S.A. Beyramabadi, A. Morsali, M.J. Khoshkholgh, A.A. Esmaeili, N, N′-dipyridoxyl Schiff bases: synthesis, experimental and theoretical characterization, Spectrochim. Acta. Part A 83 (2011) 467–471.

[59] C. Lee, W. Yang, R.G. Parr, Development of the Colle-Salvetti correlation-energy formula into a functional of the electron density, Phys. Rev. B 37 (1988) 785.

[60] M. Frisch, G. Trucks, H. Schlegel, G. Scuseria, M. Robb, J. Cheeseman, J. Montgomery Jr., T. Vreven, K. Kudin, J. Burant, Gaussian 03, Revision B. 05, Gaussian, Inc., Pittsburgh, PA, 2003, p. 12478.

[61] P.J. Hay, W.R. Wadt, Ab initio effective core potentials for molecular calculations. Potentials for K to Au including the outermost core orbitals, J. Chem. Phys. 82 (1985) 299–310.

[62] D.C. Young, Computational Chemistry: a Practical Guide for Applying Techniques to Real World Problems, Wiley Online Library, New York, 2001.

[63] G. Zhurko, D. Zhurko, ChemCraft, Version 1.7, URL, 2009, http://www.chemcraftprog.com.

[64] S. Beyramabadi, A. Morsali, A. Shams, N, N′-dipyridoxyl (1, 2-diaminocyclohexane) and its Cu (II) complex: synthesis, experimental and theoretical studies, J. Struct. Chem. 56 (2015) 243–249.

[65] H. Eshtiagh-Hosseini, M.R. Housaindokht, S.A. Beyramabadi, S.H.M. Tabatabaei, A.A. Esmaeili, M.J. Khoshkholgh, Synthesis, experimental and theoretical characterization of N, N′-dipyridoxyl (1, 4-butanediamine) Schiff-base ligand and its Cu (II) complex, Spectrochim. Acta. Part A 78 (2011) 1046–1050.

[66] T. Toozandejani, S.A. Beyramabadi, H. Chegini, M. Khashi, A. Morsali, M. Pordel, Synthesis, experimental and theoretical characterization of a Mn (II) complex of N, N′-dipyridoxyl (1, 2-diaminobenzene), J. Mol. Struct. 1127 (2017) 15–22.

[67] J.D. Crane, L.C. Emeleus, D. Harrison, P.A. Nilsson, A non-symmetrical compartmental ligand derived from acetazolamide and its mononuclear cobalt (III) complex with an empty outer compartment, Inorg. Chim. Acta 357 (2004) 3407–3412.

[68] N.V. Tverdova, E.D. Pelevina, N.I. Giricheva, G.V. Girichev, N.P. Kuzmina, O.V. Kotova, Molecular structure of N, N′-o-phenylene-bis (salicylideneaminato) copper (II) studied by gas-phase electron diffraction and quantum-chemical calculations, Struct. Chem. 22 (2011) 441–448.

[69] N. Tverdova, E. Pelevina, N. Giricheva, G. Girichev, N. Kuzmina, O. Kotova, Molecular structures of 3d metal complexes with various Schiff bases studied by gas-phase electron diffraction and quantum-chemical calculations, J. Mol. Struct. 1012 (2012) 151–161.

[70] D. Ware, D. Mackie, P. Brothers, W. Denny, Synthesis and characterization of cationic bis-aziridine cobalt (III) complexes containing schiff base ligands, Polyhedron 14 (1995) 1641–1646.

[71] M.B. Gzaiel, A. Oueslati, I. Chaabane, M. Gargouri, Density functional theory calculations of the molecular structure and the vibrational spectra of bis-tetrapropyl-ammonium hexachloro-dizincate, J. Mol. Struct. 1122 (2016) 280–289.

[72] Z. Moosavi-Tekyeh, N. Dastani, Intramolecular hydrogen bonding in N-salicylideneaniline: FT-IR spectrum and quantum chemical calculations, J. Mol. Struct. 1102 (2015) 314–322.

[73] G. Mariappan, N. Sundaraganesan, FT-IR, FT-Raman spectra, density functional computations of the vibrational spectra, molecular geometry, conformational stability and some molecular properties of 1-Bromo-2, 3-dimethoxynaphthalene, J. Mol. Struct. 1074 (2014) 51–61.

[74] R. Mathammal, K. Sangeetha, M. Sangeetha, R. Mekala, S. Gadheeja, Molecular structure, vibrational, UV, NMR, HOMO-LUMO, MEP, NLO, NBO analysis 3, 5 di tert butyl 4 hydroxy benzoic acid, J. Mol. Struct. 1120 (2016) 1–14.

[75] Y.B. Alpaslan, H. Gökce, G. Alpaslan, M. Macit, Spectroscopic characterization and density functional studies of (Z)-1-[(2-methoxy-5-(trifluoromethyl) phenylamino) methylene] naphthalene-2 (1H)-one, J. Mol. Struct. 1097 (2015) 171–180.

[76] J. Sanmartin, A.M. Garcia-Deibe, M. Fondo, D. Navarro, M.R. Bermejo, Synthesis and crystal structure of a mononuclear iron (III)(η 2-acetato) complex of a β-cis folded salen type ligand, Polyhedron 23 (2004) 963–967.

[77] N. Tverdova, N. Giricheva, G. Girichev, N. Kuz'mina, O. Kotova, A. Zakharov, IR Spectra of N, N′-Ethylene-Bis (salicylaldiminates) and N, N′-ethylene-Bis (acetylacetoniminates) of Ni (II), Cu (II), and Zn (II), Russ. J. Phys. Chem. A 83 (2009) 2255–2265.

[78] A. Kanaani, D. Ajloo, G. Grivani, A. Ghavami, M. Vakili, Tautomeric stability, molecular structure, NBO, electronic and NMR analyses of salicylideneimino-ethylimino-pentan-2-one, J. Mol. Struct. 1112 (2016) 87–96.

[79] X.-Z. Lian, Y. Huang, Y.-Q. Li, W.-J. Zheng, A green synthesis of tetrahydrobenzo [b] pyran derivatives through three-component condensation using N-methylimidazole as organocatalyst, Monatsh. für. Chem. Mon. 139 (2008) 129–131.